Macromolecules

Article

pubs.acs.org/Macromolecules

Polymer Brush-Functionalized Surfaces with Reversible, Precisely Controllable Two-Way Responsive Wettability

Wei Sun, Shouxue Zhou, Bo You, and Limin Wu*

Department of Materials Science and State Key Laboratory of Molecular Engineering of Polymers, Advanced Coatings Research Center of MEC, Fudan University, Shanghai 200433, China

ABSTRACT: This paper is the first to present a facile method of fabricating intelligent surfaces with reversible, precisely controllable, two-way responsive wettability. The ABC-type block copolymers of *tert*-butyl methacrylate (*t*BMA), 2-hydroxyethyl methacrylate (HEMA), and 2-(diisopropylamino)ethyl methacrylate (DPAEMA) were synthesized through living radical polymerization mediated by a reversible addition−fragmentation chain transfer (RAFT) process and then grafted onto acyl chloride group-functionalized SiO_2 films to produce V-shaped PDPAEMA-*b*-PHEMA-*b*-P*t*BMA brush-grafted SiO_2 films. After hydrolysis, V-shaped polymer brushes with two arms of PDPAEMA and PMAA were produced. Because the PMAA and PDPAEMA segments were highly and independently responsive to pH values, the as-obtained films not only exhibited reversible, one-to-one, precisely controllable wettability but also two-way response behavior as pH value increased.

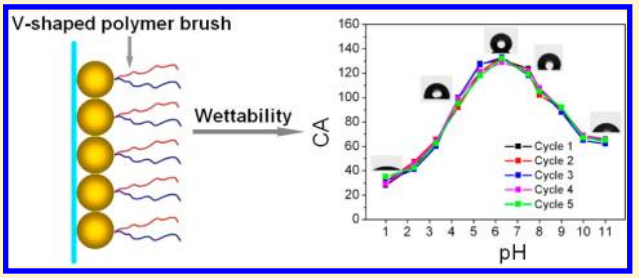

INTRODUCTION

One new approach to the development of smart materials is the preparation of stimulus-responsive surfaces whose physicochemical properties can be reversibly changed depending on different external stimuli. Smart surfaces with reversibly switchable wettability are of great importance in both academic research and practical applications.[1−3]

Currently, there are many wettability-tunable materials that can be switched between superhydrophobicity and superhydrophilicity under different stimuli such as pH,[4−6] UV light irradiation,[7−10] thermal treatment,[11,12] solvent,[13−15] electric fields,[16,17] and multiple stimuli.[18−20] However, very few reports have addressed the fabrication of materials whose wettability can be precisely controlled by the intensity of an external stimulus. In fact, materials with precisely controllable wettability have many important potential applications. For example, for stimulus-modulated porous membranes, superhydrophobicity and superhydrophilicity only be switched on and off. The velocity of an electric current can be closely controlled if the wettability of the conductive materials can be made to respond precisely to external stimuli. This on/modulate/off system would be absolutely superior to the current on/off systems, especially in situations that require fine control of the conditions. However, although two-way responsive systems are more interesting and more important than the one-way responsive systems in some fields, most of the stimulus-responsive surfaces described in previous reports have only shown a one-way stimulus response. That is, the stimulus-responsive surfaces only became more hydrophilic with increasing pH[4] or UV irradiation[7,8] or decreasing temperature[11,12] and vice versa.[5,6] Although Minko et al. observed a case of specific two-way pH-responsive wettability by sequence grafting of poly(*tert*-butyl acrylate) and poly(2-vinylpyridine) onto silicon wafers,[21] the controllability over the surface wettability was weak, and the change in water contact angle was less than 50° due to the properties of the grafted polymers and substrates. No surface with reversible, precisely controllable, two-way responsive wettability has yet been reported.

Generally, the preparation of smart surfaces with reversible, precisely controllable, two-way responsive wettability is extremely difficult to accomplish solely through simple blending (based on the chemical group transition of the surfaces). This is because it is almost impossible to control the degree of group transition quantitatively. Recently, grafting of stimuli-responsive polymer brushes to the surfaces of these materials has been shown to be an effective and versatile means of producing smart materials or surfaces with specific properties.[22−28] Stimulus-responsive polymers can simultaneously control surface energy and topography under the influence of external stimuli, and the bound state of polymer brushes can also provide thermal and solvent stability under various processing conditions.[29] However, it has been established that the structure and conformation of copolymer brushes have an important impact on their properties.[30,31] So far, polymer bushes in the shape of block copolymers,[32,33] binary brush layers,[34−36] hyperbranched polymers,[37,38] and nanoparticle-embedded polymer layers[39,40] have all been fabricated. Specifically, the grafting of Y-shaped binary copolymer brushes of A and B with relatively high molecular weights randomly tethered to a solid surface resulted in a dramatic structural reorganization and specific responsive to external stimuli.[26] Tsukruk et al. fabricated Y-shaped molecules

Received: July 6, 2013
Revised: August 11, 2013
Published: August 26, 2013

   dx.doi.org/10.1021/ma401416k | *Macromolecules* 2013, 46, 7018−7026

Scheme 1. Synthesis of Triblock Copolymers

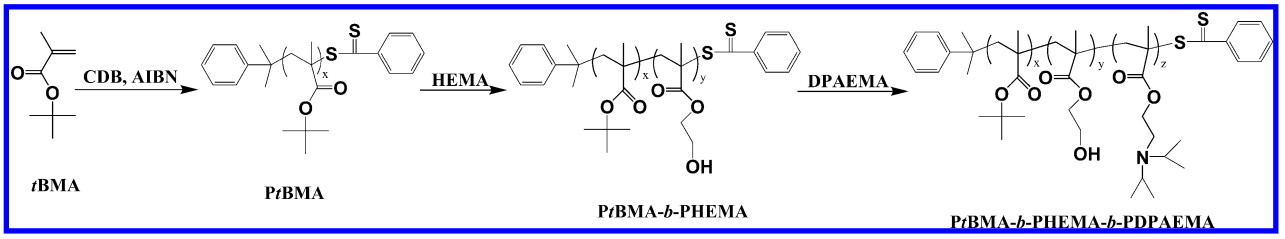

of two incompatible polymer chains (polystyrene and poly(*tert*-butyl acrylate)) attached to a functional stemlike segment capable of covalent grafting to functionalized silicon surfaces.[41−43] Novel nanoscale surface structures of segregated pinned micelles and craterlike micelles formed by grafted copolymer brushes and their reversible reorganization in selective solvents were observed. They further prepared surface-grafted nanoscale layers consisting of Y-shaped binary molecules with one polystyrene arm and one poly(acrylic acid) arm each. A bimodal distribution of elastic modulus arising from the mixed chemical composition of topmost layer was observed. This resulted in dramatic variation in friction and wear properties after exposure to different solvents.[44] Tonhauser et al. prepared silicon surfaces functionalized by Y-shaped block copolymer brushes with dissimilar polymer chains of polystyrene and poly(ethylene oxide). They used covalent binding of TEOS, and reversible stimulus-responsive surface wetting behavior was observed due to the reversible reorganization of the polymer brushes.[45] However, these Y-shaped polymer brush-functionalized surfaces only presented changes in water contact angles less than 30°, although theoretical stimulation showed such Y-shaped binary polymer brushes with arms of moderate length could form a wide variety of segregated surface layers controlled by the chemical attachment of chains A and B according to theoretical stimulation.[46]

In this study, we have for the first time prepared a novel V-shaped polymer brush-functionalized surface. Compared with previous reported Y-shaped polymer brushes, which needed several steps of coupling reaction and were covalently linked to the surface with only one in-chain anchor group, in the V-shaped polymer brushes, the triblock copolymers reported here were obtained by sequence RAFT polymerization and grafted onto the surface by a multi point-to-point grafting reaction. Thus, this method can increase the grafting efficiency and simplify the preparation procedure. This functional film was prepared by grafting ABC-type block copolymers of *tert*-butyl methacrylate (*t*BMA), 2-hydroxyethyl methacrylate (HEMA), and 2-(diisopropylamino)ethyl methacrylate (DPAEMA) onto acyl chloride-functionalized SiO_2 film. The center-linking approach allowed the attachment of V-shaped polymer brushes on the surface of the film surface to be highly and independently responsive to changes in pH. Compared to previously reported materials with switchable wettability, the polymer brush-functionalized films produced in this way not only showed reversible responses but also presented precisely controllable wettability in response to pH, specifically two-way responsive wettability in response to increasing pH.

EXPERIMENTAL SECTION

Materials. *t*BMA (Aladdin, ≥99%) and HEMA (Aladdin, ≥99%) were distilled before use. DPAEMA (Aldrich, ≥99%) was passed through a basic alumina column before use. Benzene (≥99%), tetrahydrofuran (THF, 99.5%), dichloromethane (99.5%), *N*,*N*-dimethylformamide (DMF, 99%), and toluene (99.5%) were purchased from Sinopharm Chemical Reagent Corp. and was refluxed and distilled over sodium (Na) or CaH_2 before use. Cumyl dithiobenzoate (CDB, 98.0%) was prepared as described previously.[47] Thionyl chloride, trifluoroacetic acid (TFA), azodiisobutyronitrile (AIBN, 98%), sodium hydroxide (NaOH, 96%), hydrochloric acid (HCl, 36−38% aqueous solution), and absolute ethanol were purchased from Sinopharm Chemical Reagent Corp. Succinic anhydride (98%), (2,3-epoxypropoxy)propytrimethoxysilane (EPS), 3-aminopropyltriethoxysilane (APS), poly(ethylene imine) (PEI, 99%), and SiO_2 nanoparticles with mean dimeters of 15 nm were purchased from Aladdin. Poly(diallyldimethylammonium chloride) (PDDAC, 20 wt % aqueous solution) and poly(styrenesulfonate) (PSS, 20 wt % aqueous solution) were purchased from Aldrich. These materials were used as received.

Synthesis of Triblock Copolymers PDPAEMA-*b*-PHEMA-*b*-P*t*BMA. The triblock copolymers were synthesized using sequence-controlled radical polymerization mediated by a RAFT process, as shown in Scheme 1. First, a solution of AIBN (0.0164 g, 0.1 mmol), CDB (0.136 g, 0.5 mmol), and *t*BMA (2.8 g, 20 mmol) in benzene (3.0 mL) was degassed in three freeze−pump−thaw cycles and then thermostated at 60 °C in a nitrogen atmosphere for 12 h ($M_{n,GPC}$ = 3.9 × 10^3 g/mol and M_w/M_n = 1.17). Then HEMA (1.3 g, 10 mmol) was added to the system with a syringe, and the reaction was performed for another 2 h and then quenched with liquid nitrogen to produce diblock copolymers with $M_{n,GPC}$ = 5.1 × 10^3 g/mol and M_w/M_n = 1.18. The resultant diblock copolymer was used as the macromolecular chain transfer (macro-CTA) to initiate the polymerization of DPAEMA as follows: A solution of DPAEMA (2.1 g, 10 mmol), macro-CTA (0.2 g, 0.04 mmol), and AIBN (0.003 g, 0.02 mmol) in benzene (3.0 mL) was degassed in three freeze−pump−thaw cycles and allowed to react at 60 °C under a nitrogen atmosphere for 48 h and then quenched with liquid nitrogen to obtain triblock copolymers with $M_{n,GPC}$ = 4.85 × 10^4 g/mol and M_w/M_n = 1.27.

Typical GPC results of the block copolymers are shown in Figure 1. A stepwise increase in molecular weight was observed, indicating a

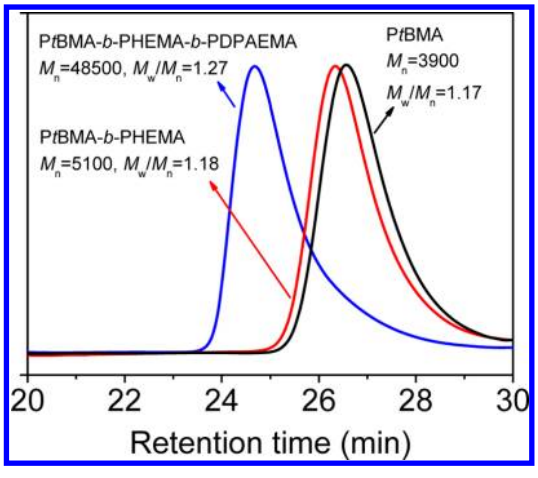

Figure 1. GPC monitoring the synthesis of triblock copolymer P*t*BMA$_{26}$-*b*-PHEMA$_{10}$-*b*-PDPAEMA$_{204}$.

dx.doi.org/10.1021/ma401416k | *Macromolecules* 2013, 46, 7018−7026

living feature of polymerization, and the molecular weight distribution of the as-obtained block copolymer was very narrow. Figure 2 shows

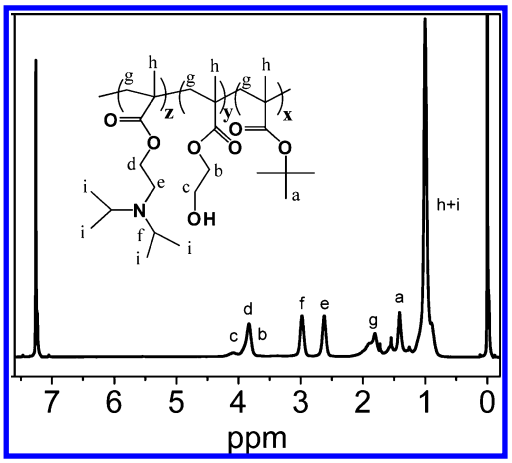

Figure 2. ^{1}H NMR spectrum of triblock copolymer P*t*BMA$_{26}$-*b*-PHEMA$_{10}$-*b*-PDPAEMA$_{204}$.

the ^{1}H NMR spectrum of the triblock copolymers. From the integrations of the *tert*-butyl signal at 1.4 ppm and the tertiary amine signal at 2.6 ppm, combined with the molecular weight of P*t*BMA, the degrees of polymerization of *t*BMA and DPAEMA were calculated to be 26 and 204, respectively.

Simply by changing the feeding mole ratios of the monomers, a series of triblock copolymers with different ratios of DPAEMA to *t*BMA were synthesized with the same method for investigation of the influence of copolymer composition on the wettability of films, as summarized in Table 1. Besides, another triblock copolymer, PHEMA-*b*-P*t*BMA-*b*-PDPAEMA, was synthesized using the same method as above but with a different charging monomer sequence to investigate the influence of copolymer structure on the wettability of the films. Its random copolymer, PHEMA-*co*-P*t*BMA-*co*-PDPAEMA, was synthesized by conventional solution polymerization for the sake of comparison. The specific parameters of these copolymers are summarized in Table 2.

Table 1. Molecular Parameters of P*t*BMA-*b*-PHEMA-*b*-PDPAEMA Triblock Copolymers Synthesized for Discussion of Effects of Copolymer Composition on the Wettability of the Surfaces

no.	sample code[a]	*t*BMA:DPAEMA	$M_{n,GPC}$	$M_{n,NMR}$[b]	M_w/M_n
1	P*t*BMA$_{26}$-*b*-PHEMA$_{10}$-*b*-PDPAEMA$_5$	5:1	5 700	6 200	1.18
2	P*t*BMA$_{26}$-*b*-PHEMA$_{10}$-*b*-PDPAEMA$_{25}$	1:1	9 600	10 500	1.22
3	P*t*BMA$_{26}$-*b*-PHEMA$_{10}$-*b*-PDPAEMA$_{53}$	1:2	15 800	16 400	1.21
4	P*t*BMA$_{26}$-*b*-PHEMA$_{10}$-*b*-PDPAEMA$_{204}$	1:8	48 500	48 700	1.27
5	P*t*BMA$_{26}$-*b*-PHEMA$_{10}$-*b*-PDPAEMA$_{309}$	1:12	67 500	71 000	1.28

[a]The numbers in subscript represent the degrees of polymerization of each segment from $M_{n,NMR}$. [b]$M_{n,NMR}$ was calculated from the integrations ratio of the *tert*-butyl signal at 1.4 ppm (belongs to P*t*BMA) and the tertiary amine signal at 2.6 ppm (belongs to PDPAEMA), combined with the molecular weight of P*t*BMA from GPC.

Table 2. Molecular Parameters of Block and Random Copolymers Synthesized for Discussion of Effects of Copolymer Structure on the Wettability of the Surfaces

no.	sample code	*t*BMA:DPAEMA	$M_{n,GPC}$	$M_{n,NMR}$	M_w/M_n
1	P*t*BMA$_{26}$-*b*-PHEMA$_{10}$-*b*-PDPAEMA$_{204}$[a]	1:8	48 500	48 700	1.27
2	PHEMA$_9$-*b*-P*t*BMA$_{25}$-*b*-PDPAEMA$_{203}$	1:8	45 500	46 200	1.28
3	PHEMA-*co*-P*t*BMA-*co*-DPAEMA	1:8[b]	29 500		4.22

[a]The numbers in subscript represent the degrees of polymerization of each segment from $M_{n,NMR}$. [b]The mole ratio of *t*BMA to DPAEMA was calculated from ^{1}H NMR.

Preparation of Acyl Chloride Group-Functionalized SiO_2 Films. SiO_2 films with a hierarchical structure were prepared using the electrostatic self-assembly method with SiO_2 nanoparticles and PDDAC deposition onto clean glass substrates at room temperature according to the literature.[8] The substrates were then incubated in 1 wt % of APS in dry toluene solution for 5 h. They were then removed from the solution and washed well in toluene to remove excess reagent. Then the substrates were held at 120 °C for 30 min and washed well in toluene and water. The as-obtained amino-SiO_2-covered substrates were then immersed into a DMF solution with 2.5 wt % succinic anhydride and kept at room temperature for 24 h. During this process, the amino groups were transferred to carboxyl groups. The carboxyl-SiO_2-covered substrates were washed with excess ethanol and dried. They were then immersed in thionyl chloride at room temperature for 24 h to introduce acyl chloride groups onto the surfaces of SiO_2 films. The substrates were finally washed with excess dichloromethane and dried in a vacuum.

Preparation of Copolymer Brush-Grafted SiO_2 Films. Triblock copolymers PDPAEMA-*b*-PHEMA-*b*-P*t*BMA were grafted onto the surfaces of SiO_2 films by the reaction of the hydroxyl groups of PHEMA and the acyl chloride groups of the functionalized SiO_2 films, as shown in Scheme 2. Typically, the acyl chloride group-functionalized SiO_2 films were immersed into a THF solution containing 2.5 wt % triblock copolymers and 0.5 wt % triethylamine. The mixture was kept at 60 °C for 24 h, and the substrates were washed with excess THF and dried in a vacuum. Then the polymer brush-grafted SiO_2 film−substrates were immersed into a dichloromethane solution containing 2 wt % TFA at room temperature for 24 h. Finally, the substrates were washed with excess dichloromethane and dried in a vacuum.

Preparation of Copolymer Brush-Covered SiO_2 Nanoparticles. The copolymer brush-covered SiO_2 nanoparticles were prepared. They served as a model for deduction of the dynamic behavior and ionization state of the grafted copolymer brushes on SiO_2 films at different pH values because it is difficult to investigate these properties of the polymer brush-grafted SiO_2 films directly. As in the fabrication of polymer brush-grafted SiO_2 films, SiO_2 nanoparticles were first functionalized with amino, carboxyl, and finally acyl chloride groups, successively. The triblock copolymers were then grafted onto the surfaces of SiO_2 nanoparticles using the reaction of hydroxyl groups with the acyl chloride groups. Finally, after hydrolysis of P*t*BMA segment, the PMAA-*b*-PHEMA-*b*-PDPAEMA brush-covered SiO_2 nanoparticles were produced.

Characterization. Water contact angle (CA) was determined using an OCA15 contact angle analyzer (Dataphysics, Germany). The substrate was first placed in solutions with specific pH values for 15 min, then removed from the solution, and blow dried with N_2. Since the neutral water could change the ionization state of these groups of polymer brushes, the water droplets (2 μL) with the same pH as the solution used for the switching were dropped carefully onto the surface of the substrate. An average CA value was produced by measuring each sample at three different positions. SEM images were scanned with a Philips XL 30 field emission microscope at an accelerating voltage of 10 kV. Atomic force microscopy (AFM) (Dimension 3100, Digital Instruments) was used to image the samples under ambient conditions in tapping mode with a silicon cantilever (40 N/m). The surface composition of the film was measured using X-ray photoelectron spectroscopy (XPS, PerkinElmer PHI 5000C ECSA) with Al K

Scheme 2. Procedure for the Preparation of V-Shaped Copolymer Brush-Grafted SiO_2 Film

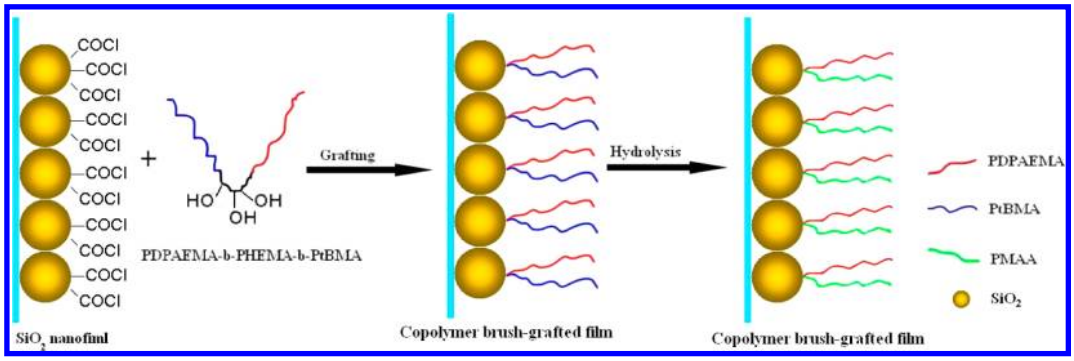

radiation at a 90° takeoff angle. All binding energy values were calibrated using the reference peak of C1S at 284.6 eV. The zeta-potentials of the samples were obtained using a zeta-potential analyzer (Zetaplus, Brookhaven Instruments Corp.) at 25 °C. ^{1}H NMR measurements were carried out on a Bruker (500 MHz) NMR instrument, using $CDCl_3$ as the solvent and tetramethylsilane as the interior reference. GPC analyses were performed at Waters calibrated by narrow polystyrene standards with a DAWN HELEOS (Wyatt multiangle laser light scattering detector, He−Ne 658.0 nm), and THF was used as the eluent at a flow rate of 1.0 mL/min at 35 °C.

RESULTS AND DISCUSSION

Fabrication of Intelligent Films. A SiO_2 film covered with V-shaped copolymer brushes was prepared by grafting of ABC-type triblock copolymers, P*t*BMA-*b*-PHEMA-*b*-PDPAEMA, onto the surfaces of SiO_2 films functionalized with acyl chloride using the reaction between the hydroxyl groups of PHEMA segment and the acyl chloride groups of SiO_2, as shown in Scheme 2. This center-linking process ensured that the as-obtained polymer brush-grafted SiO_2 film would have an exact 1:1 mole ratio of A (P*t*BMA) and C (PDPAEMA) arms. The middle PHEMA segments were fixed on the SiO_2 surfaces, leaving the A and C arms highly dissociated, which favored these two arms responding to the external stimuli independently and neatly. Considering the advantages of living characterization of RAFT process and "grafting on" strategy, the lengths of the two polymer brushes were modulated as needed simply by changing the ratios of the feeding monomers. Besides, the degree of polymerization of middle segment PHEMA was set to only 10. This allowed multiple point-to-point grafting reactions between the copolymers and the SiO_2 films, which were able to increase the grafting efficiency, and the potential cross-linking reactions between copolymers can be minimized due to the short PHEMA segment and the space hindrance.

The SEM images of the as-obtained SiO_2 film and the copolymer brush-grafted SiO_2 film are demonstrated in Figures 3a,b. The SiO_2 nanoparticles aggregated together to create the nanopores of several dozen nanometers and finally form micro- and nanopore structure which can provide sufficient surface roughness for the formation of superhydrophobic surfaces. The micro/nano-structure was retained even after grafting by copolymers. The typical AFM image of the copolymer brush-grafted SiO_2 films is shown in Figure 3c, with the root-mean-square roughness (R_{rms}) of 57.8 nm and the peak−valley distance of 301.6 nm.

The existence of copolymer layer on the SiO_2 films was further proved by XPS. As shown in Figure 4a, except for the Si and O signals, the N 1s core-level signal and the C 1s signal

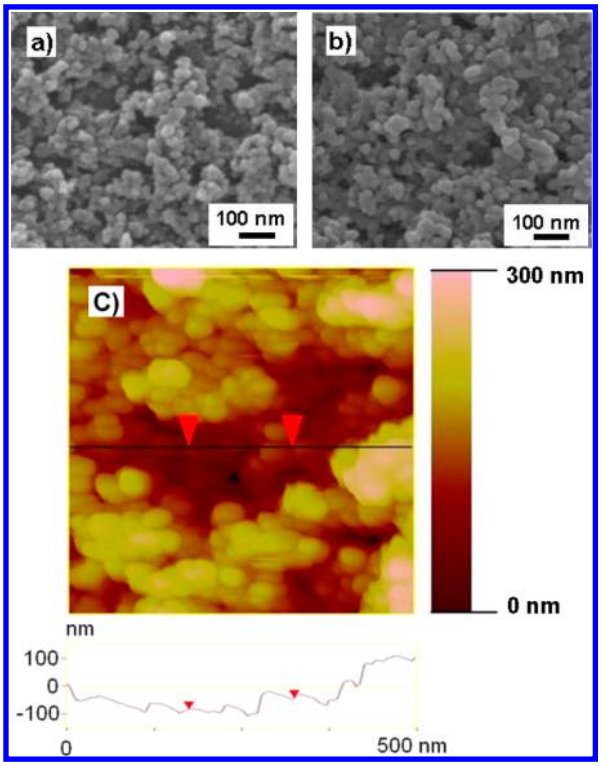

Figure 3. SEM images of the as-obtained (a) SiO_2 films and (b) SiO_2 films grafted with P*t*BMA$_{26}$-*b*-PHEMA$_{10}$-*b*-PDPAEMA$_{204}$ copolymer brushes and (c) AFM tapping mode height image of SiO_2 film grafted with P*t*BMA$_{26}$-*b*-PHEMA$_{10}$-*b*-PDPAEMA$_{204}$ copolymer brushes and cross sections of the line shown in the image.

were observed. The C 1s spectrum was further curve-fitted into four peaks using XPS differentiation imitation (with full width at half-maximum (fwhm) of 1.9 eV). As shown in Figure 4b, the fitting peaks centered at binding energies of 284.6, 285.6, 285.9, and 288.6 eV were attributed to alkyl C−C, C−N, C−OR, and O═C−O, respectively,[48] from triblock copolymers.

The wettability of the film surface was highly sensitive to pH value and could be precisely controlled between hydrophilicity and hydrophobicity by treating the surface with different pH solutions. Unlike the previously reported wettability switchable surfaces, only superhydrophobicity and superhydrophilicity state were usually obtained, few reports have focused on the middle state between superhydrophobicity and superhydrophilicity. Herin, this wettability (reflected as the contact angle) can be precisely controlled by the intensity of external stimuli. As shown in Figure 5, when the film was treated with various pH solutions, one-to-one responsive water contact angle to pH

dx.doi.org/10.1021/ma401416k | Macromolecules 2013, 46, 7018−7026

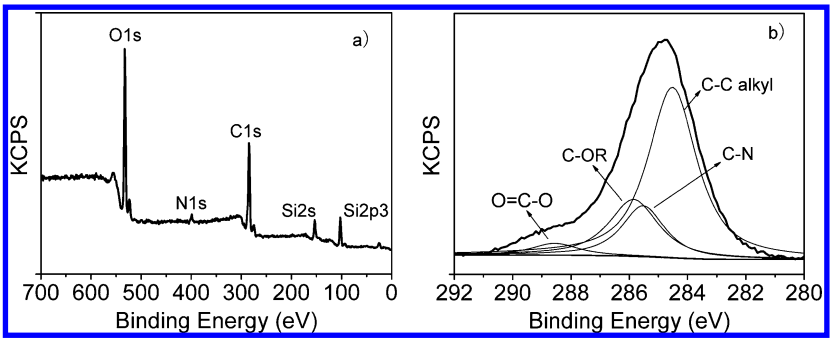

Figure 4. (a) XPS scan of SiO_2 films grafted with P*t*BMA$_{26}$-*b*-PHEMA$_{10}$-*b*-PDPAEMA$_{204}$ copolymer brushes grafted and (b) curve-fitted C 1s.

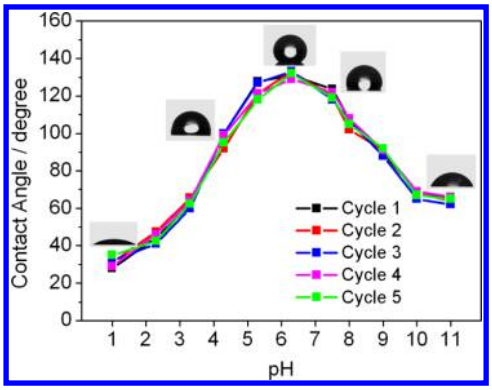

Figure 5. Reversible, precisely controllable, two-way responsive wettability of the SiO_2 films grafted with P*t*BMA$_{26}$-*b*-PHEMA$_{10}$-*b*-PDPAEMA$_{204}$ copolymer brushes treated with different pH solutions.

value was clearly visible. For example, after the surface treated with pH = 3.3 solution, the average contact angle of 63 ± 2° was obtained, and the average contact angle would change to 106 ± 3° after treated with pH 8.0 solution. The contact angle remained the same over 5 min. This process could be repeatable over several cycles, and the deviations all remained less than ±3°. These results indicated that the as-obtained triblock copolymer brush-grafted SiO_2 films all had excellent pH sensitivity and reversibility.

The films produced in this way showed a surprising two-way response to pH. As pH increased, the films showed an increasing contact angle at the initial stage. However, the contact angle started to decrease along as pH increased further. This differs considerably from previously reported wettability switchable materials, which exhibited only a one-way stimulus response.

Effects of Copolymer Composition. A series of triblock copolymers with different ratios of DPAEMA to *t*BMA were synthesized and grafted onto the SiO_2 films for investigation of the influence of copolymer composition on the wettability of films. After hydrolysis, the V-shaped polymer brushes of different ratios of DPAEMA to MAA segment-grafted SiO_2 films were produced. As shown in Figure 6a, all the V-shaped copolymer brush-grafted SiO_2 films showed two-way responsive wettability with variations in pH. The water CA increased with the concentration of DPAEMA increased. However, because the pronounced hydrophobicity of the PDPAEMA segment at high pH, too much DPAEMA reduced the controllability of CA at high pH values. However, increases in the MAA content of the polymer brush increased the hydrophilicity of surfaces at high pH values, which also decreased the extent of change of CA under pH stimulus. When PMAA dominated in the copolymer brushes, the film showed hydrophilicity within the whole pH range.

Single PDPAEMA and PMAA brush-grafted SiO_2 films exhibited only a one-way stimulus response with changes in pH, as shown in Figure 6b. This is similar to traditional materials with switchable wettability. The PDPAEMA-grafted film showed near-superhydrophilicity at low pH ranges and near-superhydrophobicity at high pH ranges, and there was a sharp increase in the contact angle between pH = 5 and 6, which may have been caused by the protonation of tertiary amine within this pH range. The PMAA-grafted film showed hydrophilicity throughout the pH range due to the high hydrophilicity of the PMAA segment.

Effects of Copolymer Structure. For the sake of comparison, triblock copolymer, PHEMA-*b*-P*t*BMA-*b*-PDPAEMA, which was synthesized with a different charging monomer sequence and its random copolymer, PHEMA-*co*-P*t*BMA-*co*-

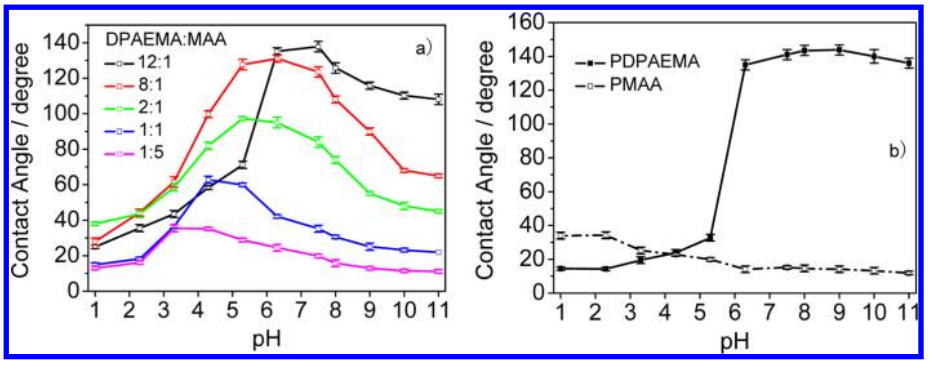

Figure 6. Wettability variation of the SiO_2 films grafted with (a) V-shaped copolymer brushes with different compositions and (b) single PDPAEMA or PMAA segments at different pH values.

dx.doi.org/10.1021/ma401416k | *Macromolecules* 2013, 46, 7018−7026

PDPAEMA, which was synthesized by conventional solution polymerization, were synthesized to investigate the influence of copolymer structure on the wettability of the films. In conventional radical polymerization, it is almost impossible to keep the distribution of molecular weight narrow. Here the mole ratio of the three monomers was kept similar to that of triblock polymer in order to investigate the effects of the structure of copolymer brushes on the wettability of the surface. After the copolymers were grafted onto the SiO_2 films and hydrolyzed with TFA, triblock copolymers PHEMA-*b*-PMAA-*b*-PDPAEMA and random copolymers PHEMA-*co*-PMAA-*co*-PDPAEMA brush-grafted SiO_2 films were produced. As shown in Figure 7, both the films grafted using these two copolymers

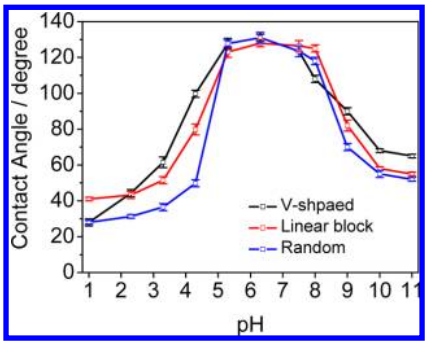

Figure 7. Wettability variation of SiO_2 films grafted with triblock copolymers triblock copolymer P*t*BMA$_{26}$-*b*-PHEMA$_{10}$-*b*-PDPAEMA$_{204}$ (forming V-shaped polymer brushes), PHEMA$_9$-*b*-P*t*BMA$_{25}$-*b*-PDPAEMA$_{203}$ (forming linear block polymer brushes), and random copolymers PHEMA-*co*-PMAA-*co*-PDPAEMA at different pH values.

also showed two-way wettability responsive to pH variation but not as high a level of sensitivity as the V-shaped block polymer brush-grafted film, indicating weakened controllability over the wettability by pH. Because the compositions of the three copolymers were similar, the difference only lies in the kinetic activity of their polymer segments. For the PMAA-*b*-PHEMA-*b*-PDPAEMA-grafted film, the HEMA segments are fixed on the SiO_2 surfaces during the grafting reaction, producing V-shaped copolymer brush-grafted film. This left the other end segments free, which produced both PMAA and PDPAEMA arms in response to the stimulus. This high sensitivity to variations in pH could render the wettability of the film surface precisely tunable by pH value. However, for the PHEMA-*b*-PMAA-*b*-PDPAEMA- or PHEMA-*co*-PMAA-*co*-PDPAEMA-grafted films, at most only one free arm remained, and the PDPAEMA and PMAA chains could not change their conformation in solution freely because of restriction by other segments. This dramatically limited the movement of the polymer segments and the sensitivity of the response of the film to changes in external pH.

Stimulus-Responsive Mechanism of the Films. The switchable wettability of surfaces was found to be highly dependent upon both the morphology and the chemical composition of surfaces. The surface morphologies of the films were scanned by SEM and found to be almost the same, indicating that switchable wettability could mainly be attributed to changes in the composition of surface chemicals rather than roughness.

The V-shaped polymer brush consisted of two relatively independent PMAA and PDPAEMA segments. As shown in Scheme 3a, PMAA segments contained −COOH groups which

Scheme 3. (a) Reversible Protonated/Deprotonated Process for PMAA and PDPAEMA Segments at Low and High pH Values;[a] (b) Changes in the Conformation of the V-Shaped Copolymer Brush-Grafted Films at Low and High pH Values

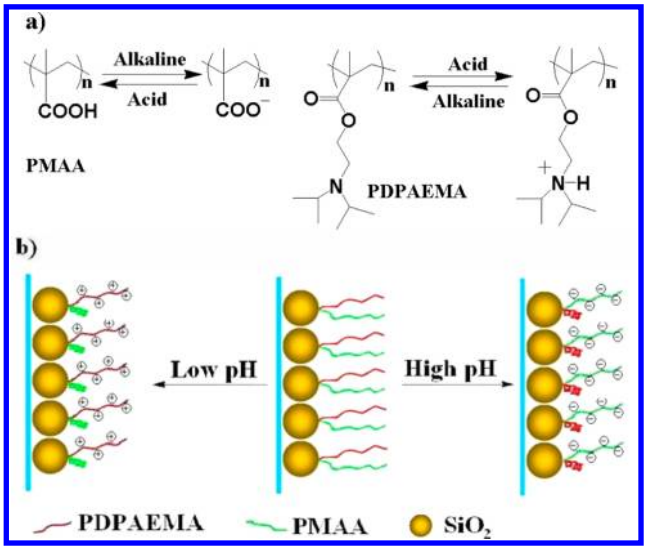

[a]The two segments exhibited opposite ionization processes.

were deprotonized upon exposure to high pH values, forming more hydrophilic −COO$^-$ groups and lowering CA. In contrast, low pH values switched the −COO$^-$ groups back to uncharged −COOH groups, which are more hydrophobic, increasing CA. The PDPAEMA segments contained ionizable tertiary amine groups, which could accept and donate protons in response to the change of pH value[6] and showed responses completely different from those of PMAA segments. At low pH values, tertiary amine groups were protonated and the electrostatic repulsion force dominated, placing polymer chains in an expanded state, decreasing CA. At high pH values, hydrophobic interactions became dominant because the ionizable groups were deprotonated, increasing CA. This rapid change in the net charge of the pendant group was found to alter the hydrodynamic volume and wettability of the polymer chain.

To assess the changes in the composition of surface groups at different pH values, the elemental composition of these surface groups was investigated using XPS. Figure 8 shows the XPS spectra of N 1s signal of the as-obtained films treated with different pH solutions. The fitting peaks centered at binding energies of 401.6 and 399.7 eV were attributed to $R_3\underline{N}^+-$ and $R_3\underline{N}$, respectively.[5] The intensity of the $R_3\underline{N}^+-$ peak was much larger than that of the $R_3\underline{N}$ peak at pH = 2 because tertiary amine groups were protonated. The inverse phenomenon occurred at pH = 5 because of the deprotonation of ionizable groups. Increases in pH to 7 or even 11 had little influence on the ratio of $R_3\underline{N}^+-$ to $R_3\underline{N}$ peaks, indicating that deprotonation had been nearly saturated at pH values higher than 5, contributing to high CA. However, as pH increased, more PMAA segments became ionized and transferred to the surface, decreasing CA at high pH. This change in the composition of surface chemicals at the topmost layer of the film was confirmed by XPS. Because the N element only existed in the PDPAEMA segment, changes in N atomic contents reflected the surface distribution of the PDPAEMA segment. After treatment with pH = 2 solution, the N atomic content increased from 1.72 to 2.59%, indicating that more PDPAEMA

dx.doi.org/10.1021/ma401416k | *Macromolecules* 2013, 46, 7018−7026

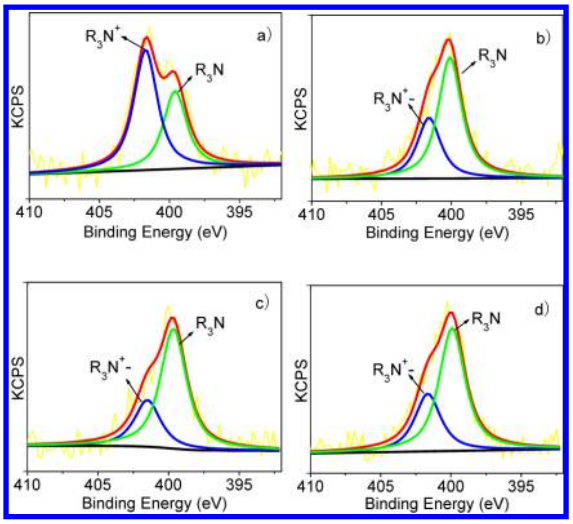

Figure 8. XPS spectra of N 1s signals of the SiO_2 films grafted with P*t*BMA$_{26}$-*b*-PHEMA$_{10}$-*b*-PDPAEMA$_{204}$ triblock copolymer brushes treated with various pH solutions: (a) 2, (b) 5, (c) 7, and (d) 11.

segments had moved to the surface after treatment with the acid solution. After these films were treated with pH = 7 solution, the N atomic content decreased to 1.95% and decreased to only 1.24% when treated with pH = 11 solution. This indicates that the higher the pH value, the more hydrophobic the PDPAEMA becomes and the fewer PDPAEMA segments move to the surface. Correspondingly, more PMAA chains were transferred to the surface when pH was high. These opposite responses of PMAA and PDPAEMA segments give the triblock copolymer brush-grafted film a maximum water CA and a two-way responsive wettability with the variations in pH. Because of the V-shaped copolymer brushes, these two highly independent polymer segments can change their morphology in the dispersion freely and respond to changes in pH. However, random or linear copolymer-grafted films showed little sensitivity to pH because the segments were bound to the substrates.

For pH-responsive wettability, not only the chemical composition but also the ionization state and conformation of the polymer chains at topmost layers at different pH values are very important.[1−3] However, because it is difficult to determine the ionization state and conformation of the polymer brushes on the films directly, the zeta-potentials of the copolymer brush-grafted SiO_2 nanoparticles were measured at different pH values. This allowed observation of the ionization state and conformation of the grafted copolymer brushes and the mechanism of pH-responsive wettability of the films.

As shown in Figure 9a, the pure SiO_2 nanoparticles exhibited a negative charge throughout the pH range. Because of the solution properties of carboxyl and tertiary amine groups, the SiO_2 nanoparticles showed an even more negative charge after grafting by PMAA, but the PDPAEMA-grafted SiO_2 particles showed a positive charge throughout the whole pH range, indicating that, after the grafting reaction, the zeta-potential of the nanoparticles was mainly determined by the grafted polymer brushes. For PDPAEMA-grafted nanoparticles, the lower the pH value, the greater the positive charge of the zeta-potential, and the more hydrophilic PDPAEMA. Correspondingly, the PDPAEMA-grafted film showed near-superhydrophilicity when pH was low and near-superhydrophobicity when pH was high. However, the CA of PMAA-grafted film showed the opposite trend.

Figure 9b shows the relationship between pH values and the zeta-potential of SiO_2 nanoparticles grafted with V-shaped copolymer brushes with different compositions. The grafted polymer brushes assembled into different morphologies at different pH values, and the zeta-potentials were mainly determined by the polymer segments assembled at the topmost layer.[49] As shown in Figure 9b, all nanoparticles exhibited a positive charge at low pH and a negative charge at high pH. There was an isoelectric point for each type of nanoparticle. This isoelectric point increased as DPAEMA content increased due to the positive charge of the PDPAEMA segment. Generally, there were two different forces driving the supramolecular organization of V-shaped amphoteric copolymer brushes.[49,50] The first is electrostatic interaction between positively and negatively charged units, and the other is hydrophobic interactions. Because of the specific V-shape of the structure, each polymer segment maintained a highly independent kinetic mobility and kept its free response to pH values. At the molecular level, the pH-responsive property of each polymer chain in the copolymer brush became amplified to macro level as the controllable wettability became highly sensitive to pH. Because the pK_a values of PMAA and PDPAEMA are 5.35 and 6.3, respectively,[6,51] at very low pH values, the tertiary amine groups became highly ionized and

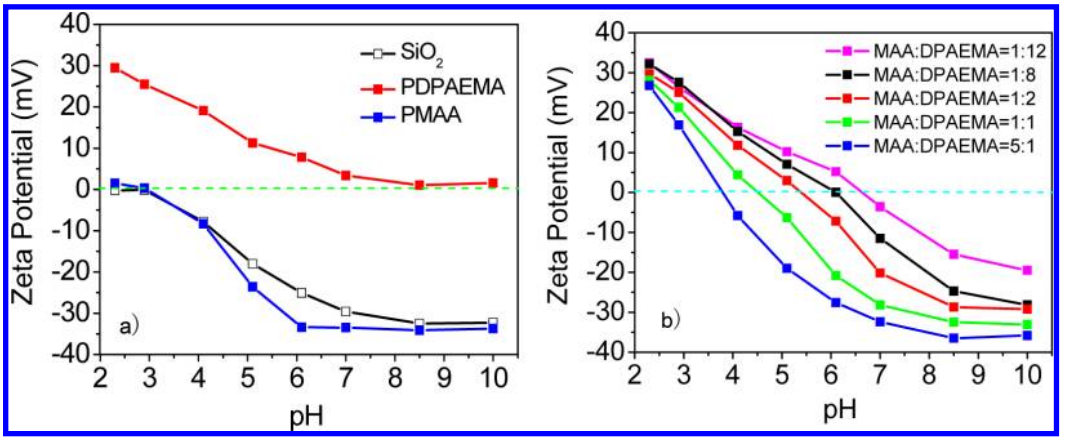

Figure 9. Relationship between pH value and zeta-potential of SiO_2 nanoparticles grafted with (a) PDPAEMA, PMAA, or no polymer and (b) V-shaped copolymer brushes with different compositions.

dx.doi.org/10.1021/ma401416k | *Macromolecules* 2013, 46, 7018−7026

hydrophilic and the carboxyl groups remained uncharged. The uncharged PMAA segments, which had compact and collapsed macromolecular chains, tightened inside the copolymer brushes because of the hydrophobic interactions while the hydrophilic PDPAEMA had a loosely coiled conformation and stretched on the surfaces of films.[52,53] This rendered the zeta-potential of the nanoparticles highly positive. As pH increased, some of the PMAA blocks became ionized, and the electrostatic interactions between these negative units and the positively charged PDPAEMA blocks took place together. The positive charge decreased as pH increased, which decreased the zeta-potential of the surface. When the pH reached the isoelectric point, the net charge of the copolymer brush was zero, and the polymer brushes entered their most compact and collapsed state. The strong electrostatic interactions between the oppositely charged blocks dominated, and the lack of uncompensated free charges results in the highly hydrophobic copolymer brushes.[49] As pH increased further, the uncompensated negative charges of the PMAA units began to spread along the surface, and more uncharged PDMAEMA blocks transferred to the core due to the hydrophobic interaction. Electrostatic interactions were gradually replaced with hydrophobic ones as pH increased with the concomitant release of the negatively charged PMAA segments from the micellar core to the surface, increasing the negative charge at the surface.

Figures 9b and 6a show that at certain pH values the larger the absolute value of zeta-potential, the more hydrophilic the copolymer at topmost layer, corresponding to the lower CA of this copolymer brush-grafted SiO_2 films. As a result, the film presented the largest CA near the pH value at the isoelectric point. For example, the isoelectric point of $PMAA_{26}$-*b*-PHEMA-*b*-$PDPAEMA_{204}$-grafted SiO_2 nanoparticles (PMAA:PDPAEMA = 1:8) was about 6.2 (Figure 9b), which corresponded to the pH at which $PMAA_{26}$-*b*-PHEMA-*b*-$PDPAEMA_{204}$-grafted SiO_2 films exhibited their largest CA (pH = 6.3, CA = 135°, Figure 5). Starting from the isoelectric point, the absolute value of zeta-potential increased as pH increased or decreased, resulting in specific two-way responsive wettability in the copolymer-grafted SiO_2 films through adjustment of pH value. These highly independent and opposite responses of V-shaped copolymer brushes of PMAA and PDPAEMA segments to pH values variation provided the triblock copolymer-grafted SiO_2 films with precisely controllable two-way responsive wettability to pH values.

CONCLUSION

Highly sensitive pH-responsive films were fabricated by grafting V-shaped polymer brushes onto SiO_2 films. The water CA of the films produced in this way exhibited not only reversible and one-to-one responsiveness but also two-way responsive behavior as pH increased. This means that the wettability of the as-obtained films can be reversibly and precisely controlled in two directions by adjusting the pH. This specific switchable wettability can be attributed to changes in the ionization state and free conformation of the highly independent PMAA and PDPAEMA brushes in response to changes in pH. Such wettability switchable materials may have applications in fields such as microfluidic switching, surfactants, smart coatings, and oil−water separation. Besides, due to the wide applicability of monomers for RAFT polymerization, this general method can be extended to the fabrication of other smart stimulus-responsive films with specific wettability or other interesting properties.

AUTHOR INFORMATION

Corresponding Author

*E-mail: lmw@fudan.edu.cn.

Notes

The authors declare no competing financial interest.

ACKNOWLEDGMENTS

Financial support was received from the National Natural Science Foundation of China (Grants 51133001 and 21074023), National "863" foundation, the Science and Technology Foundation of Ministry of Education of China (IRT0911, 20110071130002), and Science and Technology Foundation of Shanghai (12 nm0503600, 13JC1407800).

REFERENCES

(1) Feng, X.; Jiang, L. *Adv. Mater.* **2006**, *18*, 3063−3078.
(2) Xia, F.; Jiang, L. *Adv. Mater.* **2008**, *20*, 2842−2858.
(3) Xin, B.; Hao, J. *Chem. Soc. Rev.* **2010**, *39*, 769−782.
(4) Yu, X.; Wang, Z.; Jiang, Y.; Shi, F.; Zhang, X. *Adv. Mater.* **2005**, *17*, 1289−1293.
(5) Zhang, Q.; Xia, Fan.; Sun, T.; Song, W.; Zhao, T.; Liu, M.; Jiang, L. *Chem. Commun.* **2008**, 1199−1201.
(6) Stratakis, E.; Mateescu, A.; Barberoglou, M.; Vamvakaki, M.; Fotakisae, C.; Anastasiadis, S. H. *Chem. Commun.* **2010**, *46*, 4136−4138.
(7) Feng, X.; Zhai, J.; Jiang, L. *Angew. Chem., Int. Ed.* **2005**, *44*, 5115−5118.
(8) Lim, H.; Han, J.; Kwak, D.; Jin, M.; Cho, K. *J. Am. Chem. Soc.* **2006**, *128*, 14458−14459.
(9) Caputo, G.; Cortese, B.; Nobile, C.; Salerno, M.; Cingolani, R.; Gigli, G.; Cozzoli, P. D.; Athanassiou, A. *Adv. Funct. Mater.* **2009**, *19*, 1149−1157.
(10) Kettunen, M.; Silvennoinen, R. J.; Houbenov, N.; Nykanen, A.; Ruokolainen, J.; Sainio, J.; Pore, V.; Kemell, M.; Ankerfors, M.; Lindstrom, T.; Ritala, M.; Ras, R. H. A.; Ikkala, O. *Adv. Funct. Mater.* **2011**, *21*, 510−517.
(11) Sun, T.; Wang, G.; Feng, L.; Liu, B.; Ma, Y.; Jiang, L.; Zhu, D. *Angew. Chem., Int. Ed.* **2004**, *43*, 357−360.
(12) Zhang, X.; Guo, Y.; Zhang, P.; Wu, Z.; Zhang, Z. *ACS Appl. Mater. Interfaces* **2012**, *4*, 1742−1746.
(13) Minko, S.; Müller, M.; Motornov, M.; Nitschke, M.; Grundke, K.; Stamm, M. *J. Am. Chem. Soc.* **2003**, *125*, 3896−3900.
(14) Lim, H.; Lee, S.; Lee, D.; Lee, D.; Lee, S.; Cho, K. *Adv. Mater.* **2008**, *20*, 4438−4441.
(15) Qing, G.; Wang, X.; Fuchsn, H.; Sun, T. *J. Am. Chem. Soc.* **2009**, *131*, 8370−8371.
(16) Shiu, J. Y.; Chen, P. *Adv. Funct. Mater.* **2007**, *17*, 2680−2686.
(17) Chang, J.; Hunter, I. *Macromol. Rapid Commun.* **2011**, *32*, 718−723.
(18) Xia, F.; Feng, L.; Wang, S.; Sun, T.; Song, W.; Jiang, W.; Jiang, L. *Adv. Mater.* **2006**, *18*, 432−436.
(19) Xia, F.; Ge, H.; Hou, Y.; Sun, T.; Chen, L.; Zhang, G.; Jiang, L. *Adv. Mater.* **2007**, *19*, 2520−2524.
(20) Sun, W.; Zhou, S.; You, B.; Wu, L. *J. Mater. Chem. A* **2013**, *1*, 3146−3154.
(21) Ionov, L.; Houbenov, N.; Sidorenko, A.; Stamm, M.; Luzinov, I.; Minko, S. *Langmuir* **2004**, *20*, 9916−9919.
(22) Minko, S.; Kiriy, A.; Gorodyska, G.; Stamm, M. *J. Am. Chem. Soc.* **2002**, *124*, 3218−3219.
(23) Hoy, O.; Zdyrko, B.; Lupitskyy, R.; Sheparovych, R.; Aulich, D.; Wang, J.; Bittrich, E.; Eichhorn, K.-J.; Uhlmann, P.; Hinrichs, K.; Muller, M.; Stamm, M.; Minko, S.; Luzinov, I. *Adv. Funct. Mater.* **2010**, *20*, 2240−2247.
(24) Stuart, M. A. C.; Huck, W. T. S.; Genzer, J.; Muller, M.; Ober, C.; Stamm, M.; Sukhorukov, G. B.; Szleifer, I.; Tsukruk, V. V.; Urban, M.; Winnik, F.; Zauscher, S.; Luzinov, I.; Minko, S. *Nat. Mater.* **2010**, *9*, 101−113.

(25) Chen, T.; Ferris, R.; Zhang, J.; Ducker, R.; Zauscher, S. *Prog. Polym. Sci.* **2010**, *35*, 94−112.
(26) Liu, F.; Urban, M. W. *Prog. Polym. Sci.* **2010**, *35*, 3−23.
(27) Zhang, J.; Han, Y. *Chem. Soc. Rev.* **2010**, *39*, 676−693.
(28) Lin, X.; He, Q.; Li, J. *Chem. Soc. Rev.* **2012**, *41*, 3584−3593.
(29) Park, J.; Thomas, E. L. *J. Am. Chem. Soc.* **2002**, *124*, 514−515.
(30) Hadjichristidis, N.; Iatrou, H.; Pitsikalis, M.; Mays, J. *Prog. Polym. Sci.* **2006**, *31*, 1068−1132.
(31) Hirao, A.; Sugiyama, K.; Yokoyama, H. *Prog. Polym. Sci.* **2007**, *32*, 1393−1438.
(32) Liu, F.; Urban, M. W. *Prog. Polym. Sci.* **2010**, *35*, 3−23.
(33) Berezkin, A. V.; Guseva, D. V.; Kudryavtsev, Y. V. *Macromolecules* **2012**, *45*, 8910−8920.
(34) (a) Ionov, L.; Minko, S.; Stamm, M.; Gohy, J. F.; Jerome, R.; Scholl, A. *J. Am. Chem. Soc.* **2003**, *125*, 8302−8306. (b) Sun, W.; Zhou, S.; You, B.; Wu, L. *J. Mater. Chem. A* **2013**, *1*, 10646−10654.
(35) Lemieux, M.; Usov, D.; Minko, S.; Stamm, M.; Shulha, H.; Tsukruk, V. V. *Macromolecules* **2003**, *36*, 7244−7255.
(36) Houbenov, N.; Minko, S.; Stamm, M. *Macromolecules* **2003**, *36*, 5897−5901.
(37) Peleshanko, S.; Tsukruk, V. V. *J. Polym. Sci., Polym. Phys.* **2012**, *50*, 83−100.
(38) Ye, X.; Jiang, X.; Yu, B.; Yin, J.; Vana, P. *Biomacromolecules* **2012**, *13*, 535−541.
(39) Minko, S. *Polym. Rev.* **2006**, *46*, 397−420.
(40) Luzinov, I.; Minko, S.; Tsukruk, V. V. *Soft Matter* **2008**, *4*, 714−725.
(41) Julthongpiput, D.; Lin, Y.; Teng, J.; Zubarev, E. R.; Tsukruk, V. V. *J. Am. Chem. Soc.* **2003**, *125*, 15912−15921.
(42) Julthongpiput, D.; Lin, Y.; Teng, J.; Zubarev, E. R.; Tsukruk, V. V. *Langmuir* **2003**, *19*, 7832−7836.
(43) Lin, Y.; Teng, J.; Zubarev, E. R.; Shulha, H.; Tsukruk, V. V. *Nano Lett.* **2005**, *5*, 491−495.
(44) LeMieux, M.; Lin, Y.; Cuong, P.; Ahn, H.; Zubarev, E. R.; Tsukruk, V. V. *Adv. Funct. Mater.* **2005**, *15*, 1529−1540.
(45) Tonhauser, C.; Golriz, A. A.; Moers, C.; Klein, R.; Butt, H.-J.; Frey, H. *Adv. Mater.* **2012**, *24*, 5559−5563.
(46) Zhulina, E.; Balazs, A. C. *Macromolecules* **1996**, *29*, 2667−2673.
(47) Le, T. P. T.; Moad, G.; Rizzardo, E.; Thang, S. H. PCT International Patent Application WO 9801478 A1 980115, 1998.
(48) Yuan, W.; Jiang, G.; Wang, J.; Wang, G.; Song, Y.; Jiang, L. *Macromolecules* **2006**, *39*, 1300−1303.
(49) Gohy, J.-F.; Creutz, S.; Garcia, M.; Mahltig, B.; Stamm, M.; Jérôme, R. *Macromolecules* **2000**, *33*, 6378−6387.
(50) Cohen Stuart, M. A.; Besseling, N. A. M.; Fokkink, R. G. *Langmuir* **1998**, *14*, 6846−6849.
(51) Merle, Y. *J. Phys. Chem.* **1987**, *91*, 3092−3098.
(52) Liu, S.; Weaver, J. V. M; Tang, Y.; Billingham, N. C.; Armes, S. P. *Macromolecules* **2002**, *35*, 6121−6131.
(53) Harada, A.; Kataoka, K. *Science* **1999**, *283*, 65−67.